

Limitations of Essential-State Models for the Description of Two-Photon Absorption Processes: The Example of Bis(dioxaborine)-Substituted Chromophores[†]

Egbert Zojer,^{*,‡,§,||} Wim Wenseleers,^{‡,⊥} Peter Pacher,^{‡,§} Stephen Barlow,^{‡,||} Marcus Halik,[‡] Cara Grasso,[‡] Joseph W. Perry,^{‡,||} Seth R. Marder,^{‡,||} and Jean-Luc Bredas^{‡,||}

Department of Chemistry, The University of Arizona, Tucson, Arizona 85721-0041, Institut für Festkörperphysik, Technische Universität Graz, Petersgasse 16, A-8010 Graz, Austria, Department of Chemistry and Biochemistry, Georgia Institute of Technology, Atlanta, Georgia 30332-0400, and Physics Department, University of Antwerp (UIA), Universiteitsplein 1, B-2610 Antwerpen (Wilrijk), Belgium

Received: September 15, 2003; In Final Form: December 15, 2003

We report spectroscopic and quantum-chemical investigations comparing the two-photon absorption (TPA) properties of a bis(dioxaborine)-substituted derivative of biphenyl with those of a bis(dioxaborine) carbazole derivative. The former molecule is close to linear and centrosymmetric, while the dioxaborine groups of the latter are in a V-shaped arrangement, due to their linkage to the 3 and 6 positions of the bridging group. For both systems, we find sizable TPA cross sections (on the order of $360\text{--}530 \times 10^{-50} \text{ cm}^4 \text{ s/photon}$). Interestingly, while the TPA response in the biphenyl-based system can be well described on the basis of the traditional three-state model, a significantly larger number of excited states needs to be considered for the carbazole derivative. We present a detailed comparison of the convergence of the theoretical approaches and an analysis of the various channels that contribute to the TPA response in molecules with low effective symmetries.

I. Introduction

Over the past few years, two-photon absorption (TPA) in organic materials has attracted considerable attention due to a number of possible applications exploiting the 3D selectivity of nonlinear absorption processes, including 3D microfabrication¹ and 3D fluorescence microscopy.² Additionally, nonlinear absorbers are attractive for optical-limiting purposes.³ To optimize the materials used in these applications, a better understanding of the relationship between the chemical structure of a chromophore and its TPA cross section (δ) is essential.

To achieve this goal, synthetic and spectroscopic efforts have, in many cases, been supported and guided by quantum-chemical simulations.^{4–6} The theoretical description of the TPA response is usually based on a perturbative treatment of the frequency-dependent nonlinear optical response⁷ by calculating the imaginary part of the second-order hyperpolarizability γ^8 or on a direct evaluation of the TPA tensor, \mathbf{S} .^{9,10} In principle, the calculation of both $\text{Im}(\gamma)$ and \mathbf{S} require a summation over all eigenstates of the unperturbed Hamiltonian. However, convergence of the nonlinear optical constants is usually observed upon including only a finite number of states.¹¹ Convergence can actually be expected to be faster for TPA than for hyperpolarizabilities due to the resonant nature of the nonlinear absorption process.

To be able to relate the calculated and measured trends to a small number of microscopic parameters such as transition energies and transition dipoles, approximate expressions for γ or \mathbf{S} have been developed. These are similar to the essential-state models developed for the calculation of hyperpolarizability.

In noncentrosymmetric molecules, TPA into the strongly one-photon-allowed state is usually modeled using a two-state approach; the description of TPA in centrosymmetric molecules relies in many cases on a three-state approach, including a single dominant one-photon state as an intermediate (for details, see the methodology section). These approximations are usually also applied in *ab initio* studies for which the calculation of a large number of excited states can be difficult. It has already been pointed out by Cronstrand et al.¹⁴ that, for symmetrically donor-substituted stilbene derivatives, a second intermediate state can contribute significantly, requiring the replacement of the three-state approach by a four-state approach.

In the present contribution, we compare the convergence behavior for an acceptor– π –acceptor system (4,4'-(9,10-dihydrophenanthrene-2,7-diyl)-di(6-*n*-propyl-2,2-difluoro-1,3,2-(2*H*)-dioxaborine), chromophore **I**, and an acceptor–donor–acceptor chromophore (4,4'-(*N*-*n*-hexylcarbazole-3,6-diyl)-di(6-*iso*-propyl-2,2-difluoro-1,3,2-(2*H*)-dioxaborine), chromophore **II**, see insets in Figures 1 and 2. In both cases, dioxaborines (DOBs) serve as acceptor groups; while they are linked to the central bridging unit in positions *para* with respect to the C–C bond between the two arylene moieties in **I**, they are attached to the carbazole unit in positions *meta* with respect to the C–C bond linking the two arylene groups in **II**. Therefore, **I** adopts a quasilinear roughly centrosymmetric arrangement of the two DOB groups, while **II** is V shaped. The TPA properties of chromophore **I** are well described by the usually employed few-state models, but for compound **II**, a multitude of channels is found to contribute to the TPA response. It should also be pointed out that, apart from these fundamental aspects, these chromophores are promising candidates for practical applications. For example, **II** has been applied as an efficient sensitizer for the deposition of 3D metallic silver lines.¹⁵ Thus, an in-depth understanding of their TPA response is highly desirable.

[†] Part of the special issue "Alvin L. Kwiram Festschrift".

* Author to whom correspondence should be addressed. E-mail: egbert.zojer@chemistry.gatech.edu.

[‡] The University of Arizona.

[§] Technische Universität Graz.

^{||} Georgia Institute of Technology.

[⊥] University of Antwerp.

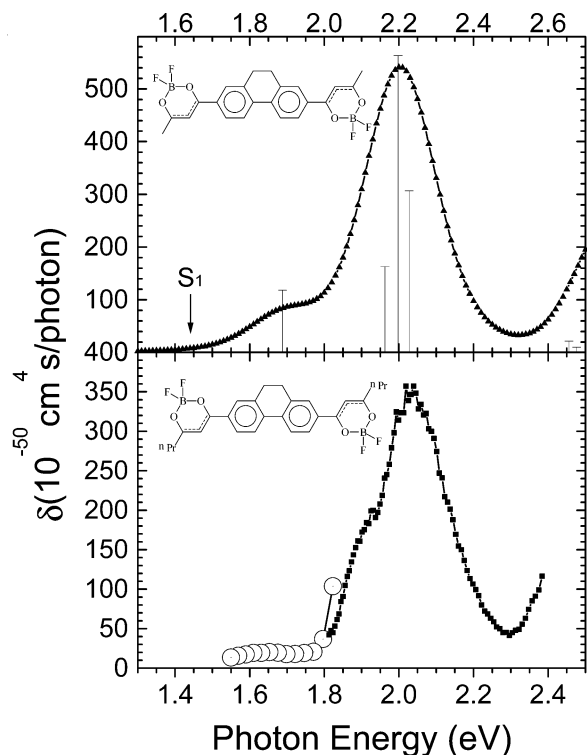


Figure 1. Calculated (top) and measured (bottom) TPA cross-sections of compound **I** as a function of the energy of the incident photons. The vertical bars in the upper graph correspond to the δ peak values calculated using the TPA tensor (δ_{TEN}), while the continuous line is derived from $\text{Im}(\gamma)$ (δ_{SOS}). The data points in the low-energy region of the bottom graph, represented by large circles, were obtained with the femtosecond laser system, while the data represented by small (solid) squares were measured with the nanosecond optical parametric amplifier. Note that the energy axes of the two plots are shifted by 0.2 eV to ease the comparison between theoretical and experimental results.

II. Experimental and Theoretical Methodology

Details for the synthesis and characterization of compound **I** are provided as Supporting Information, while the corresponding information for compound **II** has previously appeared (see supplementary information in ref 15). The molecules investigated experimentally contain *n*-propyl (**I**) or *iso*-propyl (**II**) chains on the DOB units; in **II**, the nitrogen atom bears an *n*-hexyl group; these alkyl groups are replaced by methyl groups in the calculations.

TPA spectra were obtained by the two-photon-induced fluorescence (TPF) method,¹⁶ using either 6-ns pulses (10 Hz) from an optical parametric amplifier (Spectra-Physics MOPO) or 100-fs pulses (82 MHz) from a mode-locked Ti-sapphire laser (Spectra-Physics Tsunami) for excitation.^{5,6} In these experiments, the TPF intensity is determined as a relative measure of the product of the TPA cross section δ and the fluorescence quantum efficiency η , and it is assumed that the quantum efficiencies after two-photon excitation are the same as those after one-photon excitation. The TPA cross sections are then obtained by calibration against a compound with known $\eta\delta$ product (coumarin 307 in methanol for the femtosecond measurements,¹⁶ *p*-bis-(*o*-methylstyryl)benzene (bis-MSB) in cyclohexane^{16,17} for the nanosecond experiments at $\lambda < 710$ nm, and fluorescein in aqueous NaOH solution (pH 11)¹⁶ for nanosecond pulses at $\lambda > 710$ nm).¹⁸ The samples were dissolved in dichloromethane (Aldrich, spectrophotometric grade) at concentrations of $\sim 1\text{--}2 \times 10^{-6}$ M (femtosecond measurements) and $\sim 0.5\text{--}1 \times 10^{-5}$ M (nanosecond measurements). To ensure that the measured signals were solely due to

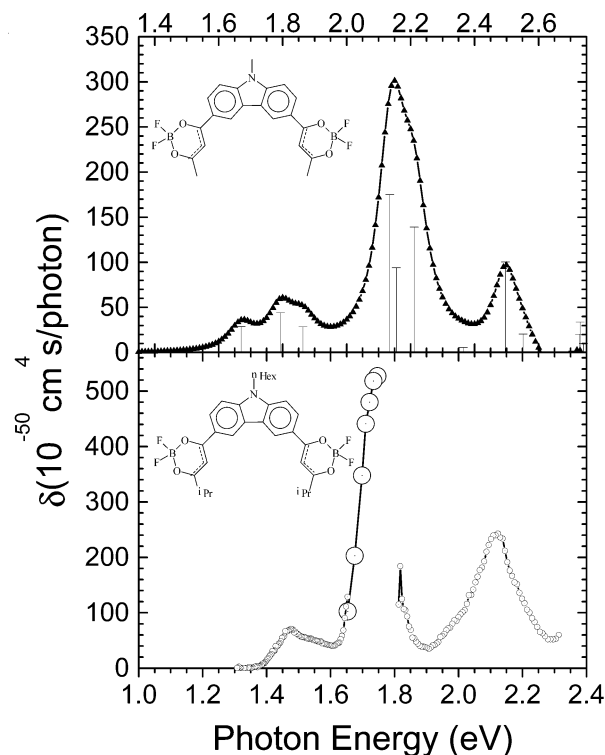


Figure 2. Calculated (top) and measured (bottom) TPA cross-sections of compound **II** as a function of the energy of the incident photons. The vertical bars in the upper graph correspond to the δ peak values calculated using the TPA tensor (δ_{TEN}), while the continuous line is derived from the $\text{Im}(\gamma)$ (δ_{SOS}). The data points represented by large circles in the bottom graph were obtained with the femtosecond laser system, while the data represented by small circles were measured with the nanosecond optical parametric amplifier. Note that the energy axes of the two plots are shifted by 0.35 eV to ease the comparison between theoretical and experimental results.

TPA, the dependence of TPF on the incident intensity was verified in each case to be quadratic.

Fluorescence quantum yields (QYs) were determined using a Spex Fluorolog 3 fluorometer with 9,10-diphenylanthracene in cyclohexane as a reference standard ($\Phi_{\text{fl}} = 70\%$ for nondeoxygenated solvent).¹⁹ The determined QYs are 72% for molecule **I** and 65% for molecule **II**.

To calculate the TPA cross sections, we started from molecular geometries optimized with the semiempirical AM1 Hamiltonian.²⁰ We note that the DOB substituents are twisted relative to the dihydrophenanthrene or carbazole cores. Thus, several conformers can exist that belong to different symmetry groups and have significantly different state dipole moments. For the analogue of compound **I** in which dihydrophenanthrene is replaced by a biphenyl unit,²¹ we have, therefore, extensively tested the influence of the molecular conformation on the predicted TPA response. We found only a minor effect on the TPA cross sections and virtually no influence on the position of the TPA maxima. For the results discussed below, the conformations used were similar to those depicted in Figures 1 and 2 with the rings in **I** twisted in a chiral manner and in **II** twisted such that the molecule adopts C_s symmetry (compare with Supporting Information).

Excited-state energies, state dipoles, and transition dipole moments were obtained by coupling the intermediate neglect of differential overlap (INDO)²² Hamiltonian to a multireference determinant single- and double-excitation configuration interaction (MRDCI)²³ scheme using the Mataga-Nishimoto potential²⁴

to express the Coulomb repulsion term. (Details concerning the chosen CI active space are available as Supporting Information.)

III. Evaluation of the TPA Cross Section

The TPA cross sections were evaluated from the imaginary part of the second hyperpolarizability γ , using the perturbative sum-over-states (SOS) approach²⁵ (δ_{SOS}), including the electronic coupling among the 300 lowest-lying excited states. Alternatively, we also calculated the TPA response using the TPA tensor S_e (δ_{TEN}).⁹ In fact, it can be shown²⁶ that for TPA into a particular excited state, both approaches become equivalent (unless one approaches the double-resonance limit with the two-photon active state at nearly twice the energy of the one-photon resonance, as will be briefly discussed below). In the following, we will, therefore, give only the mathematical expressions for δ_{TEN} , as these are more straightforward to interpret than the more complex expression for γ_{SOS} given in ref 25. Deviations between δ_{SOS} and δ_{TEN} will be discussed when appropriate.

For degenerate TPA to a particular two-photon excited state $|e'\rangle$ (i.e., the simultaneous absorption of two photons from one monochromatic laser beam), S_e is given by⁹

$$S_e^{i,j} = \sum_e \left(\frac{M_{ge}^i M_{ee'}^j}{E_{ge} - E_{ge'}/2} + \frac{M_{ge}^j M_{ee'}^i}{E_{ge} - E_{ge'}/2} \right) \quad (1)$$

M_{ge} and $M_{ee'}$ are the transition dipoles between the ground state $|g\rangle$ and an intermediate state $|e\rangle$ and between $|e\rangle$ and $|e'\rangle$, respectively. E_{ge} and $E_{ge'}$ are the corresponding transition energies. i and j refer to the Cartesian coordinates. Also here, unless otherwise stated, 300 intermediate states are considered in our calculations. In an isotropic medium and for a linearly polarized excitation source, S_e is related to the corresponding TPA cross section via^{10,27}

$$\bar{\delta}_{\text{TEN}}^{e'} = \frac{3L^4}{2n^2 c^2 \epsilon_0 \hbar} \frac{1}{15} \left(\frac{E_{ge'}}{2} \right)^2 \sum_{ij} (S_e^{ii} S_e^{*jj} + 2S_e^{ij} S_e^{*ji}) \quad (2)$$

L is the local field factor and n the refractive index of the medium.²⁸ Combining the cross sections from eq 2 for all TPA-active states $|e'\rangle$ with normalized line-shape functions yields the TPA response. The line-shape functions are chosen to be Lorentzians with the full widths at half maximum (fwhm) identical to twice the damping Γ used in the SOS approach.

In the top parts of Figures 1 and 2, we show the results derived from the SOS approach (δ_{SOS}) as continuous lines. Originally, we assume a damping factor Γ of 0.1 eV in accordance with previous studies.⁴ The vertical lines denote the energies of the TPA-active states and the lengths of these lines correspond to the peak values for TPA into the particular state $|e'\rangle$, as derived from S_e . For compound **II**, this yields calculated spectral features with widths comparable to those seen spectroscopically. For compound **I**, the experimentally observed TPA peaks are, however, significantly broader than the calculated ones, which can be mainly attributed to vibronic effects.²⁹ To account for these effects, we have convoluted the calculated δ_{SOS} in compound **I** with a normalized Gaussian function, whose width has been chosen to be 0.165 eV to match the fwhm of the experimental spectra.

The approximate expressions usually derived from eqs 1 and 2 for a Lorentzian line-shape function with a fwhm of Γ are (assuming that a single one-photon state $|e\rangle$ dominates the linear absorption):

(i) for TPA into the one-photon state in noncentrosymmetric molecules

$$\delta_{2\text{-state}} = K_1 \frac{L^4}{n^2 c^2 \epsilon_0 \hbar} \frac{M_{ge'}^2 \Delta\mu_{ge'}^2}{\Gamma} \quad (3)$$

(ii) for TPA into higher-lying states, which are not dipole-coupled to the ground state

$$\delta_{3\text{-state}} = K_2 \frac{L^4}{n^2 c^2 \epsilon_0 \hbar} \frac{M_{ge}^2 M_{ee'}^2}{(E_{ge} - E_{ge'}/2)^2 \Gamma} \quad (4)$$

$\Delta\mu_{ge}$ is the change in state dipole moment. K_1 and K_2 are numerical factors, whose actual value depends on the relative orientation of the change in state dipole and the transition dipole moments.¹⁴ Equation 3 is obtained from the two terms in eq 1 for which $e = g$ and $e = e'$; eq 4 is derived if a single intermediate state $|e\rangle$ is included and $\Delta\mu_{ge'}$ or $M_{ge'}$ are negligible. It is usually applied to describe TPA in centrosymmetric molecules. Equation 3 is frequently referred to as the two-state model and is related to the dipolar term³⁰ (D-term). Equation 4 is called the three-state approach and is related to the so-called two-photon term (T-term). As pointed out in ref 14, effective values have to be used for $M_{ee'}$ (and also $\Delta\mu_{ge}$), if these quantities are not parallel to the M_{ge} direction.

IV. Results and Discussion

The TPA spectra of compounds **I** and **II** are shown in Figures 1 and 2, respectively. The spectrum measured for **I** is dominated by a single maximum at 2.03 eV with a shoulder around 1.92 eV. In the low-energy region, we find a weak peak at 1.65 eV. The nature of the excited states involved will be briefly discussed below and is described in detail in ref 21 for similar molecules. Above 2.3 eV, δ starts to rise again and one can expect significant cross sections upon approaching a double-resonance situation. For chromophore **II**, we find three pronounced peaks at 1.48 eV, around 1.75 eV, and at 2.12 eV. Here, the investigation of the main maximum is complicated by the tuning gap of the nanosecond-MOPO laser. The achieved maximum cross section of $527 \times 10^{-50} \text{ cm}^4 \text{ s/photon}$ lies in the range of previously studied highly efficient TPA chromophores.⁴

At this point, it has to be noted that a simple comparison of peak values can sometimes be misleading; while the maximum cross section is more than 30% higher in **II** than in **I**, the integrated TPA response for the main peaks is in fact larger in chromophore **I** (an exact quantification is difficult because of the missing data points around the main maximum in **II**). This is a consequence of the different peak widths observed in the two materials. From a practical point of view, whether wide or narrow TPA features are to be preferred depends on the particular application and the frequency tuneability of the available lasers.

In general, we find a very good overall agreement between the measured and calculated data; the main difference is an overestimation of the excited-state energies by the quantum-chemical calculations. As far as the theoretical studies are concerned, the results for δ_{SOS} (lines) and δ_{TEN} (bars) are virtually identical (bearing in mind that additional broadening has been applied to δ_{SOS} in Figure 1).

The only deviations are found in the region above 2.6 eV in Figure 2, where one-photon resonant contributions to $\text{Im}(\gamma)$ render δ_{SOS} negative. This is related to the fact that $\text{Im}(\gamma)$ and,

consequently, δ_{SOS} contain not only TPA contributions, but depend on the overall nonlinear absorption cross section, as can be shown for instance by solving the damped nonlinear wave equations. Thus, upon approaching the region of linear absorption, effects such as ground-state bleaching can contribute to the intensity-dependent absorption coefficient. Although terms similar to the microscopic description of ground-state bleaching can be identified in the negative resonances in the SOS description of $\text{Im}(\gamma)$, one should realize that the perturbative description we have applied (which, e.g., assumes an identical damping for all excited states) cannot provide a proper description of those effects. One of the reasons for that is that the lifetimes, which correspond to the damping factors in the SOS expression, are related to the dephasing times of the system, while ground-state bleaching is determined by the total incoherent lifetime of the S_1 state. Therefore, the description of TPA by δ_{SOS} at energies relatively close to one-photon absorption features has to be considered with care.

TPA in compound **I** is characterized by a weak peak at 1.65 eV (1.89 eV) and a strong peak at 2.03 eV (2.20 eV) in the experimental (theoretical) spectrum. As can be seen from δ_{TEN} (the bars in the upper graph), the strong peak is a superposition of two-photon excitation into several excited states. A detailed analysis of the quantum-mechanical description of the weak low-energy state and the dominant high-energy state reveals that both are dominated by single-particle excitations from the HOMO to the LUMO + 1 and from the HOMO - 1 to the LUMO. As will be discussed in more detail below, TPA in compound **I** can be reasonably well described using the three-state model. Applying eq 4, it appears that one of the main origins for the different TPA cross sections of the states at 1.89 and 2.20 eV is a larger M_{ee} for the higher-lying state. The latter can be explained by the different signs with which the (HOMO \rightarrow LUMO + 1) and the (HOMO - 1 \rightarrow LUMO) determinants enter in their CI descriptions. Such effects are discussed in detail for analogous molecules with a biphenyl and a fluorenyl (rather than dihydrophenanthrene) core in ref 21.

The situation is considerably more complex in chromophore **II** (see Figure 2); first, due to the strong deviation from a centrosymmetric structure, the strongly one-photon-allowed peaks also gain two-photon activity. An analysis of the factors determining the TPA cross sections for this molecule is further complicated by the fact that, for all analyzed excited states in compound **II**, a multitude of different channels contribute to the actual value of δ ; as a result, the essential-state models given in eqs 3 and 4 can no longer be applied. This will be discussed in more detail below.

Figure 3 shows that for both investigated chromophores δ_{TEN} has converged well upon including about 20 intermediate states. An expansion of that region is, therefore, given in Figure 4. Here, the value of $\delta/\delta_{\text{converged}}$ for zero intermediate states is defined as the contribution that originates from a change in the state dipole moment (i.e., the terms in eq 1 in which the intermediate state is either $|g\rangle$ or the target TPA state $|e\rangle$) equivalent to eq 3. Changes in state dipole upon excitation obviously make no significant contribution in chromophore **I**; this is expected, since the molecule is close to centrosymmetric. In compound **II**, this type of channel plays a significant role only for TPA into the S_1 state, which gives rise to the peak at 1.67 eV.

The inclusion of S_1 into the summation (i.e., one intermediate state in Figure 4) already accounts for most of the converged TPA into the two analyzed states in molecule **I** (S_2 and S_4 , top part of Figure 4). In fact, δ is overestimated by around 30% for

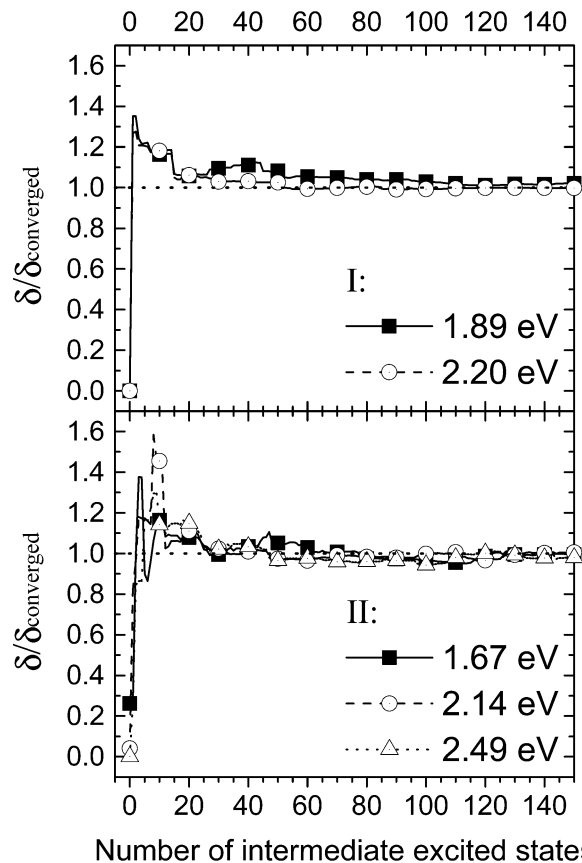


Figure 3. Evolution of the TPA-tensor calculated cross section into the most dominant excited states of chromophores **I** and **II** as a function of the number of intermediate states. An intermediate state number of 0 refers to the contribution arising from the dipolar term given in the 2-state approach in eq 3. $\delta_{\text{converged}}$ is the value obtained upon including 300 intermediate states.

the two analyzed states and gradually decreases to the converged value with the biggest steps occurring upon including the weakly one-photon-allowed S_3 and S_{15} states.

Again, the situation is considerably more complex in compound **II**. To illustrate this, we have plotted in Figure 5 the main channels giving rise to TPA into S_1 . Channel a is the contribution due to the change in state dipole mentioned above. It corresponds to including S_0 and S_1 as intermediate states in eq 1. As shown in Figure 4, the inclusion of S_2 gives rise to a significant increase of the cross section associated with TPA into S_1 . This is due to two new channels (b and c in Figure 5). Channel b is a typical T-type channel (as described by eq 4), arising from the square of the " $M_{0-2} \times M_{2-1}$ " term of the \mathbf{S} tensor (i.e., the term in which S_2 plays the role of the intermediate state $|e\rangle$). Channel c combines the " $M_{0-1} \times \Delta\mu_{0-1}$ " component of the \mathbf{S} tensor with the " $M_{0-2} \times M_{2-1}$ " component, thus mixing a contribution involving a state dipole change with one that only contains transition dipole moments. Such combinations are usually not included in the simple two-state and three-state models.

The next intermediate (one-photon-allowed) state to be considered in the summation for compound **II** is S_3 . Its inclusion results in another δ increase by about 40%. As both M_{0-3} and M_{3-1} are relatively small, the contribution from the direct combination of these transition dipoles in a T-type fashion (" $M_{0-3} \times M_{3-1}$ " \times " $M_{0-3} \times M_{3-1}$ ") is only minor. The main contributions upon including S_3 thus come from combining the new " $M_{0-3} \times M_{3-1}$ " component with the " $M_{0-1} \times \Delta\mu_{0-1}$ " and " $M_{0-2} \times M_{2-1}$ " components, giving rise to channels d and

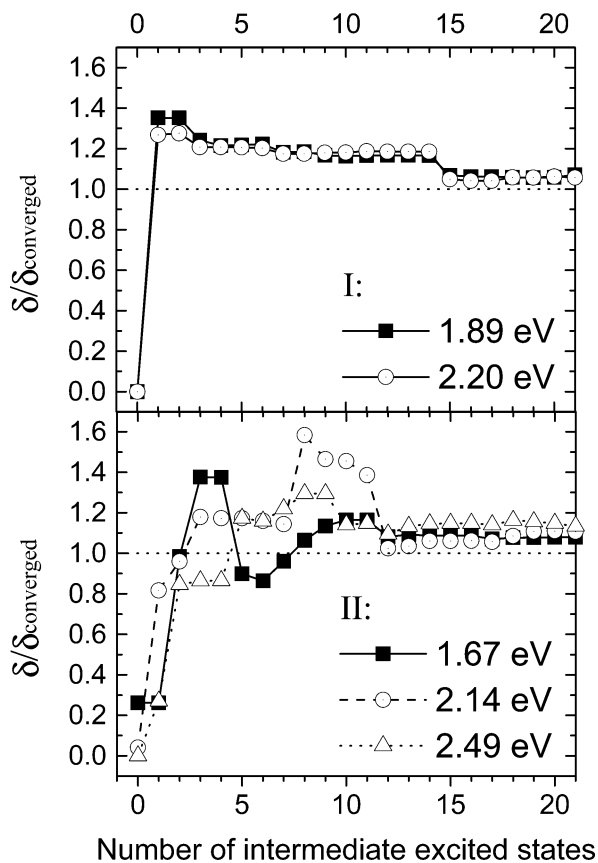


Figure 4. Evolution of δ_{TEN} in **I** and **II** when including up to 20 intermediate states into eq 1 (i.e., zoom into in Figure 3); $\delta_{\text{converged}}$ is the value obtained for including 300 intermediate states.

e in Figure 5. A property of channel e, which distinguishes it from the channels discussed before, is that it combines two different terms of the \mathbf{S} tensor, which both only contain transition dipoles. The main contributions from including the next one-photon active state (S_5) are related to channels f and g. They reduce the overall cross section due to the signs of the transition

dipoles involved. This makes channel g equivalent to the “interference term” described for the generalized four-state model in 14.

A further complication is that all channels depicted in Figure 5 result in off-diagonal elements of the TPA tensor, as at least two of the coupled transition dipoles and/or state dipole changes are orthogonal. The channels depicted in Figure 5 are those most strongly affecting δ into S_1 ; however, as shown by the evolution in Figure 4, channels involving higher-lying one-photon-allowed states also contribute.

For TPA into the next analyzed peak (S_5 at 2.14 eV), the situation is similarly complex. There, the largest component of the \mathbf{S} tensor is the one that combines the two parallel transition dipoles $M_{0 \rightarrow 1}$ and $M_{1 \rightarrow 5}$ (“ $M_{0 \rightarrow 1} \times M_{1 \rightarrow 5}$ ” term of the \mathbf{S} tensor). Thus, the single most significant channel contributing to TPA into S_5 is a T-type expression containing these two transition dipoles (reminiscent of channel b from Figure 5). There is, however, a significant number of other one-photon-allowed states (in particular S_2 , S_3 , S_8 , and S_{12}), which give rise to additional channels (see also evolution of δ in Figure 4). The most significant channels involving these states are the mixed channels of the same type as g in Figure 5, which include the “ $M_{0 \rightarrow 1} \times M_{1 \rightarrow 5}$ ” term of the \mathbf{S} tensor. For the TPA peak at 2.49 eV (S_9), one encounters a situation similar to S_5 with the main difference being that the components of the \mathbf{S} tensor involving S_1 and S_2 as intermediate states are of comparable magnitude, which gives rise to an even larger number of mixed channels with significant contributions to δ .

The discussion in the previous paragraphs indicates that the main difference between compounds **I** and **II** is that in **II** there exists a significantly larger number of moderately to strong one-photon-allowed states than in **I**; all of these have to be considered as intermediate states in eq 1. This assessment is fully supported by the linear absorption spectra of the investigated molecules, which are shown in Figure 6. While the absorption spectrum of **I** is dominated by the $S_0 \rightarrow S_1$ transition and its vibronic sidebands, one finds a large number of relatively strong peaks in chromophore **II**. This is related to the strong deviation from inversion symmetry in the molecular structure

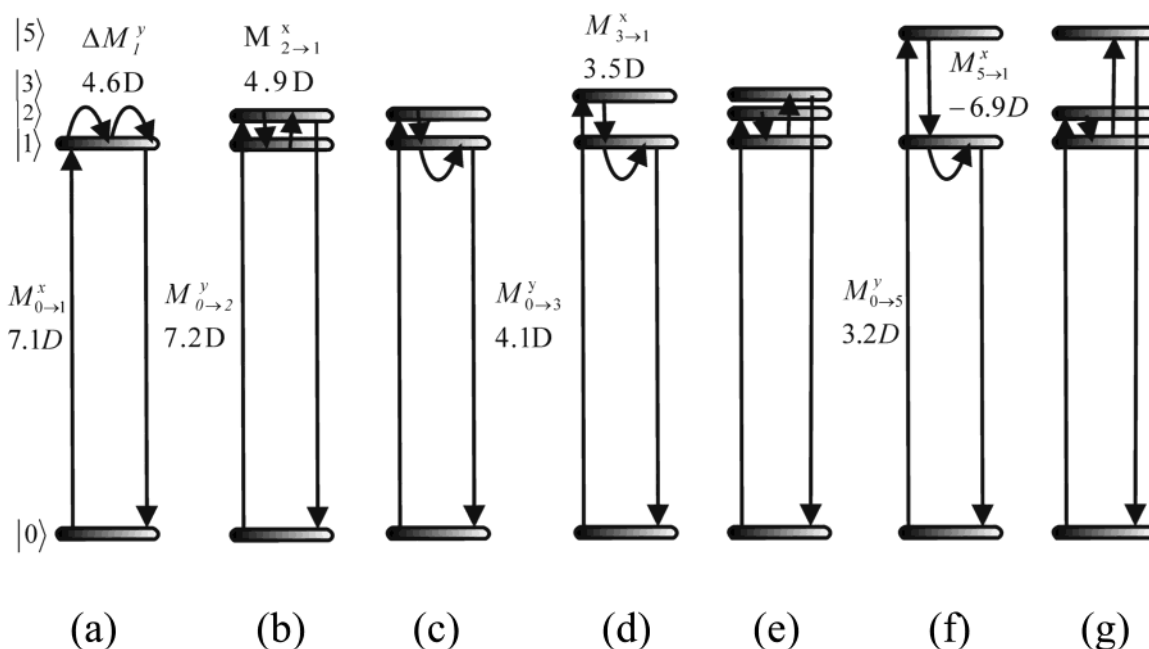


Figure 5. Sketch of the channels that most strongly contribute to TPA into the S_1 state in chromophore **II**. The horizontal bars denote the ground state $|0\rangle$ and the various excited states. The straight arrows symbolize the transition dipoles and the curved arrows the change in state dipole moment between the excited state and the ground state.

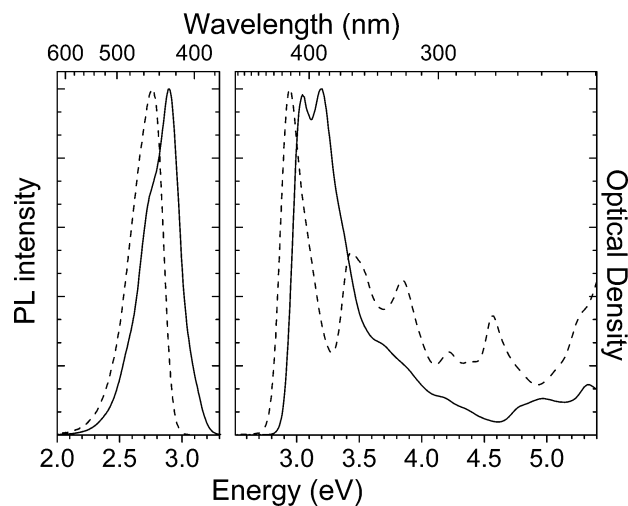


Figure 6. Normalized linear absorption and emission spectra of chromophores **I** (solid line) and **II** (dashed line).

of **II**. This demonstrates that a close inspection of the linear absorption spectrum of a material can allow one to estimate the extent to which approximate essential-state models will prove helpful in understanding the TPA response of a chromophore.

V. Summary and Conclusions

We have discussed the TPA properties of two bis(dioxaborine)-substituted chromophores, which are promising candidates for applications exploiting nonlinear absorption. The focus of the present contribution was to determine under which circumstances approximate essential-state models can be applied to analyze δ and how the convergence behavior of perturbative descriptions of TPA is influenced by properties such as the linear absorption spectrum.

We have found that the three-state model works reasonably well to understand the nonlinear optical response in the quasilinear para-substituted dihydrophenanthrene (compound **I**). However, this model fails to properly describe the second chromophore, which has a V-type shape. In this molecule, a suitably large number of one-photon-allowed intermediate states must be included for a proper theoretical treatment. Thus, care has to be taken when using essential-state models to analyze the TPA response of molecules in which a large number of excited states contributes to the linear optical response.

Acknowledgment. The authors thank V. Coropceanu for stimulating discussions. This work is based upon work supported in part by the STC program of the National Science Foundation under Agreement No. DMR-0120967, the AFOSR (F49620-02-1-0358 and F49620-99-1-0161), the Deutsche Forschungsgemeinschaft, the University of Arizona Photonics Initiative, and the IBM SUR program. W.W. is a postdoctoral fellow of the Fund for Scientific Research—Flanders (Belgium).

Supporting Information Available: Synthesis and characterization of compound **I**. Choice of the CI active space in the INDO/MRDCI calculations. This material is available free of charge via the Internet at <http://pubs.acs.org>.

References and Notes

- (1) Parthenopoulos, D. A.; Rentzepis, P. M. *Science* **1989**, *245*, 843.
- (b) Strickler, J. H.; Webb, W. W. *Opt. Lett.* **1991**, *16*, 1780. (c) Cumpston, B. H.; Ananthavel, S. P.; Barlow, S.; Dyer, D. L.; Ehrlich, J. E.; Erskine, L. L.; Heikal, A. A.; Kuebler, S. M.; Lee, I.-Y. S.; McCord-Maughon, D.;

- Qin, J.; Röckel, H.; Rumi, M.; Wu, X.-L.; Marder, S. R.; Perry, J. W. *Nature* **1999**, *398*, 51. (d) Zhou, W. H.; Kuebler, S. M.; Braun, K. L.; Yu, T. Y.; Cammack, J. K.; Ober, C. K.; Perry, J. W.; Marder, S. R. *Science* **2002**, *296*, 1106.

- (2) Denk, W.; Strickler, J. H.; Webb, W. W. *Science* **1990**, *248*, 73.
- (b) Köhler, R. H.; Cao, J.; Zipfel, W. R.; Webb, W. W.; Hansen, M. R. *Science* **1997**, *276*, 2039. (c) Miller, M. J.; Wei, S. H.; Parker, I.; Cahalan, M. D. *Science* **2002**, *296*, 1869.

- (3) Said, A. A.; Wamsely, C.; Hagan, D. J.; van Stryland, E. W.; Reinhardt, B. A.; Roderer, P.; Dillard, A. G. *Chem. Phys. Lett.* **1994**, *228*, 646. (b) Bhawalkar, J. D.; He, G. S.; Prasad, P. N. *Rep. Prog. Phys.* **1996**, *59*, 1041. (c) Ehrlich, J. E.; Wu, X. L.; Lee, Y. L.; Hu, Z. Y.; Rockel, H.; Marder, S. R.; Perry, J. W. *Opt. Lett.* **1997**, *22*, 1843.

- (4) Albota, M.; Beljonne, D.; Brédas, J. L.; Ehrlich, J. E.; Fu, J.-Y.; Heikal, A. A.; Hess, S. E.; Kogej, T.; Levin, M. D.; Marder, S. R.; McCord-Maughon, D.; Perry, J. W.; Röckel, H.; Rumi, M.; Subramaniam, G.; Webb, W. W.; Wu, X.-L.; Xu, Ch.; *Science*, **1998**, *281*, 1653.

- (5) Rumi, M.; Ehrlich, J. E.; Heikal, A. A.; Perry, J. W.; Barlow, S.; Hu, Z.; McCord-Maughon, D.; Parker, T. C.; Röckel, H.; Thayumanavan, S.; Marder, S. R.; Beljonne, D.; Brédas, J. L. *J. Am. Chem. Soc.* **2000**, *122*, 9500.

- (6) Beljonne, D.; Wenseleers, W.; Zojer, E.; Shuai, Z.; Vogel, H.; Pond, S. J. K.; Perry, J. W.; Marder, S. R.; Brédas, J. L. *Adv. Funct. Mater.* **2002**, *12*, 631.

- (7) Orr B. J.; Ward, J. F.; *Mol. Phys.* **1971**, *20*, 513.

- (8) Dick, B.; Hochstrasser, R. M.; Trommsdorff, H. P. In *Nonlinear Optical Properties of Molecules and Crystals*; Chmela, D. S., Zyss, J., Eds.; Academic Press: Orlando, FL, 1987; Vol. 2, pp 167–170.

- (9) Peticolas, W. L. *Annu. Rev. Phys. Chem.* **1967**, *18*, 233. Zalesny, R.; Bartowiak, W.; Styrz, S.; Leszczynski, J. *J. Phys. Chem. A* **2002**, *106*, 4032.

- (10) Monson P. R.; McClain W. M. *J. Chem. Phys.* **1970**, *53*, 29.

- (11) Dehu, C.; Meyers, F.; Brédas, J. L. *J. Am. Chem. Soc.* **1993**, *115*, 6198. (b) Albert, I. D. K.; Morley, J. O.; Pugh, D. *J. Chem. Phys.* **1995**, *102*, 237.

- (12) Mazumdar, S.; Duo, D.; Dixit, S. N. *Synth. Met.* **1993**, *55–57*, 3881. (b) Mazumdar, S.; Guo, F. *J. Chem. Phys.* **1994**, *100*, 1554.

- (13) Dirk, C. W.; Cheng L. T.; Kuzyk, M. G. *Mater. Res. Soc. Proc.* **1992**, *247*, 80.

- (14) Cronstrand, P.; Luo, Y.; Ågren, H. *Chem. Phys. Lett.* **2002**, *352*, 262.

- (15) Halik, M.; Wenseleers, W.; Grasso, C.; Stellacci, F.; Zojer, E.; Barlow, S.; Brédas, J. L.; Perry, J. W.; Marder, S. R. *Chem. Commun.* **2003**, 1490.

- (16) Xu, C. and Webb, W. W. *J. Opt. Soc. Am. B* **1996**, *13*, 481.

- (17) Kennedy, S. M.; Lytle, F. E. *Anal. Chem.* **1986**, *58*, 2643.

- (18) To reduce experimental noise in the reference data and to allow for arbitrary wavelength intervals, a smooth curve fit to the discrete literature data was used. As TPA reference data for coumarin 307 showed significant discrepancies between different, overlapping, wavelength regions (obtained using different laser optics), these data were piecewise scaled to eliminate discontinuities, keeping the average δ of overlapping regions constant. A sum of 4, 2, and 5 Gaussian functions was used to fit the TPA reference spectra of bis-MSB, coumarin 307, and fluorescein, respectively.

- (19) Meech, S. R. and Phillips, D. *J. Photochem.* **1983**, *23*, 193.

- (20) Dewar, M. J. S.; Zebisch, E. G.; Healy, E. F.; Stewart, J. J. P. *J. Am. Chem. Soc.* **1985**, *107*, 3902.

- (21) Zojer, E.; Wenseleers, W.; Halik, M.; Grasso, C.; Barlow, S.; Perry, J. W.; Marder, S. R.; Brédas, J. L. Submitted.

- (22) Ridley, J.; Zerner, M. *Theor. Chim. Acta* **1973**, *32*, 111. (b) Ridley, J.; Zerner, M. *Theor. Chim. Acta* **1976**, *42*, 223.

- (23) Buenker, R. J.; Peyerimhoff, S. D. *Theor. Chim. Acta* **1974**, *35*, 33.

- (24) Mataga, N.; Nishimoto, K. *Z. Phys. Chem.* **1957**, *13*, 140.

- (25) Orr, B. J.; Ward, J. F. *Mol. Phys.* **1971**, *20*, 513.

- (26) Luo, Y.; Norman, P.; Macak, P.; Ågren, H. *J. Phys. Chem. A* **2000**, *104*, 4718.

- (27) We use $\bar{\delta}$ here, as the value calculated by eq 2 (before combining the value with a line-shape function) corresponds to the integral TPA cross section into a particular excited state, while the values usually given in the literature correspond to peak values.

- (28) Our calculations are performed for molecules in the gas phase (i.e., the influence of the solvent on the molecular geometry and on transition dipoles and transition energies is not considered). Thus, L and n are set to 1.

- (29) For the S_1 state for instance, we find excited-state relaxation energies of 0.15 eV in chromophore **I** and only 0.09 eV in **II**, when optimizing the excited-state geometries by coupling the AM1 Hamiltonian to a single configuration interaction scheme including 16 occupied and 16 unoccupied orbitals.

- (30) Meyers, F.; Marder, S. R.; Pierce, B. M.; Brédas, J. L. *J. Am. Chem. Soc.* **1994**, *116*, 10703.